Powders and Grains (2005) – García-Rojo, Herrmann and McNamara (eds)
© 2005 Taylor & Francis Group, London, ISBN 0 415 38348 X

Grain crushing and critical states observed in DEM simulations

Y.P. Cheng & M.D. Bolton
Engineering Department, Cambridge University, UK

Y. Nakata
Department of Civil Engineering, Yamaguchi University, Japan

ABSTRACT: The uniqueness of critical states is investigated using the Discrete Element Method (DEM) with microspheres bonded together to represent crushable grains. Using a cubical assembly of these grains, constant-pressure and constant-volume compression tests were computed at different densities and stress-levels. The data are compared with two previous definitions of critical states. Grain crushing led to the observation that critical state voids ratios are a function not only of the current stress, but also of the maximum historic stress and of the stress-path which is followed. Grain crushing makes "critical state" an ambiguous concept.

1 INTRODUCTION

DEM can be used to study the mechanics of crushable granular materials. An element was created with about 400 crushable grains retained by rigid walls. DEM grains were formed from bonded microspheres forming rough, irregular agglomerates. Grain breakage could therefore involve either the detachment of a single microsphere (asperity damage) or the splitting of a grain.

The theories of soil plasticity following Roscoe, Schofield and others ignored particle breakage. Recent work (Cheng et al. 2003 & 2004; Cheng 2004) shows, however, that breakage is central to the elastic-plastic transition of soils. However, breakage also raises the question of the uniqueness of the Critical State Line (CSL) which is the starting point for the Cam Clay family of soil plasticity models. The role of breakage and the definition of Critical States can now be explored through DEM simulations.

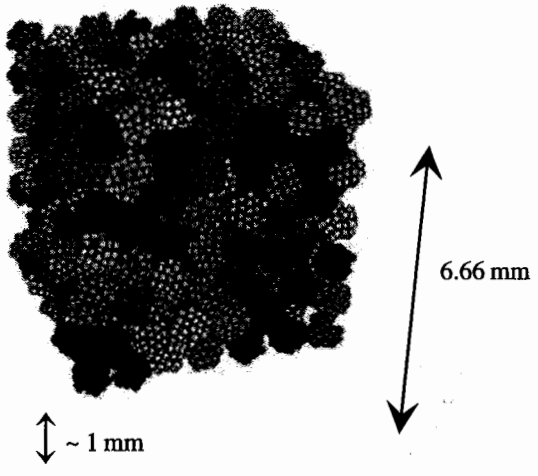

Figure 1. Cubical assembly of the DEM crushable grains.

1.1 *DEM crushable grains*

DEM crushable grains are formulated using simple contact parameters for the microspheres, namely the contact bond strength (4N) and bond stiffness (4×10^6 N/m) in normal and shear directions, and the friction coefficient (0.5) during contact sliding. The statistics of grain breakage were made to match those obtained for silica grains of similar sizes 1.4–1.7 mm. A cubical assembly of these agglomerates, Figure 1, was loaded isotropically and then axi-symmetrically. The details of how to form the DEM grains and the assemblies have been published (Robertson, 2000; Robertson & Bolton, 2001; Cheng, et al. 2003; Cheng, 2004).

1.2 *Previous definitions of critical states*

Critical States were originally defined macroscopically as ultimate states of continuous shear flow at constant volume, at which the voids ratio, e, uniquely determines both the deviator stress, q, and the mean effective (intergranular) stress, p' (Roscoe et al. 1958). Later, a different way of defining critical states was used by Schofield (1980). He considered a set of specimens all at the same voids ratio at the moment of failure during drained triaxial tests. He observed that brittle, dilatant shear ruptures occur at low pressure but that the rate of dilation decreases as p'

increases up to a critical pressure p'_{crit} beyond which the behavior changes to plastic work hardening with volumetric compression at yield. Variation of p'_{crit} with e defines what Schofield took to be a line of critical states.

1.3 *Critical stresses of sands*

Critical state soil mechanics was developed using data of clays in a framework that ignored grain crushing. Crushing during triaxial tests on sands, however, was recognized by Bolton (1986) as the cause of loss of dilatancy with increasing stress, and as the mechanism generating Schofield's critical states. Grain crushing in sands during both isotropic compression (IC) and triaxial shearing has been of increasing interest (Coop, 1990; McDowell et al. 1996; Lade et al. 1996). However, the final states in which soils were supposed to shear continuously without change in q, p' and e were very difficult to obtain even using an advanced experimental apparatus (Coop et al. 2004).

2 STRESS-STRAIN

Figure 2 shows the stress-stain data of a series of constant-p' shearing tests obtained by testing a set (Series 1) of identical DEM assemblies each with an initial voids ratio of 1.73 unstressed, each isotropically compressed to some pressure p' prior to shearing. Figure 2a shows icons marking peaks, critical pressure and final states. Figure 2b shows that shearing the DEM sample gave overall dilation at low p' and compression at high p'; $p'_{crit} \approx 9$ MPa at $e = 1.65$ for zero maximum rate of dilation.

At this critical pressure, the maximum rate of dilation reduced to zero. The arrangement-induced dilation at low stress level was compensated by the crushing-induced compression. However, the sample could not maintain the zero volume change forever. Volume started to reduce again for deviator strains in excess of 30%. This implies that the influence of breakage overrides that of rearrangement when shearing to a high strain as breakage continued.

The rate of change of volume at 60% strain was small but still perceptible. Nevertheless, Schofield's critical pressure and Roscoe et al.'s ultimate critical states clearly refer to distinctly different phenomena.

Two more series of p'-constant tests were computed: Figures 3 and 4. Figure 3 shows dilatancy data of Test Series 2 on a looser specimen with initial voids ratio 2.08 before isotropic compression. Schofield's critical pressure is estimated as $p'_{crit} = 8.5$ MPa at $e = 1.70$, similar to Test 1. Figure 4 shows data from the same initial sample but isotropically precompressed to 40 MPa, and then unloaded to various pressures for shearing at constant p' as before. These over-compressed samples dilated for $p' < p'_{crit} = 12$ MPa at $e = 1.28$.

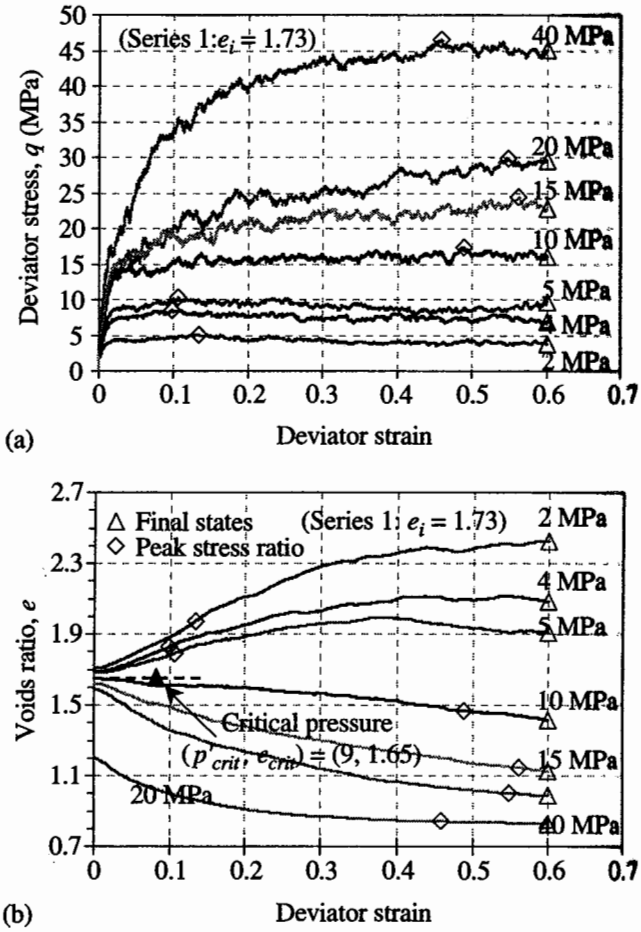

Figure 2. Critical pressure interpreted from maximum dilatancy rate (Test Series 1, ei = 1.73): (a) Deviator stress-strain curve; (b) voids ratio against deviator strain.

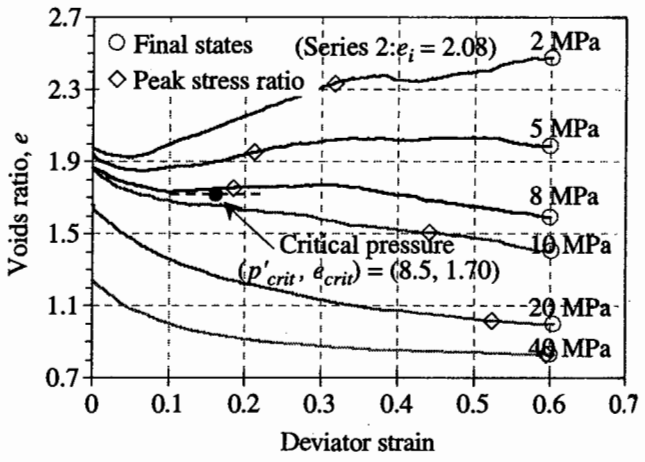

Figure 3. Critical pressure interpreted from maximum dilatancy rate (Test Series 2, $e_i = 2.08$).

3 GRAIN CRUSHING

The Weibull characteristic crushing stress at which 37% of agglomerate grains survived in individual grain compression tests was 81 MPa. Regarding the assemblies of grains, Figure 5 shows the representative particle size distribution (PSD) curves of the DEM

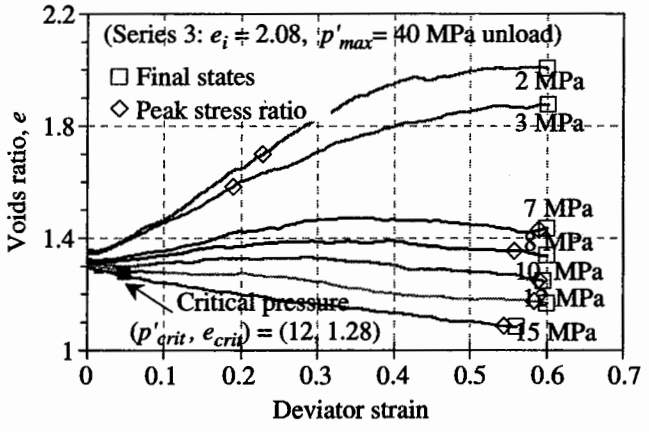

Figure 4. Critical pressure interpreted from maximum dilatancy rate (Test Series 3, ei = 2.08, p'max = 40 MPa, recompressed).

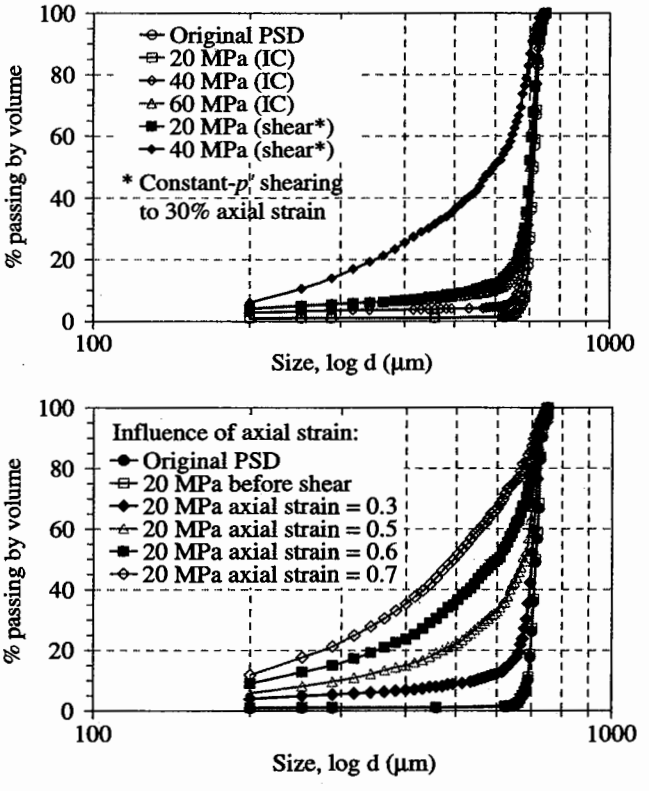

Figure 5. Particle size distribution curves (Series 2): (a) after isotropic compression; (b) after shearing (p' = 20 MPa).

assembly from Test Series 2 at various stages of loading and shearing. Figure 5a shows that during isotropic compression up to 10 MPa, the change in PSD curves was insignificant. For $p' > 20$ MPa there is degradation that inevitably leads to filling of voids. The change of PSD with shear strain, however, was much more significant. An example with shear strain at constant p' is given in Figure 5b, strongly recalling real sand experiments (Lade et al. 1996). Although there is very little change in deviator stress after 30% deviator strain, Figure 5b shows very significant degradation in the PSD.

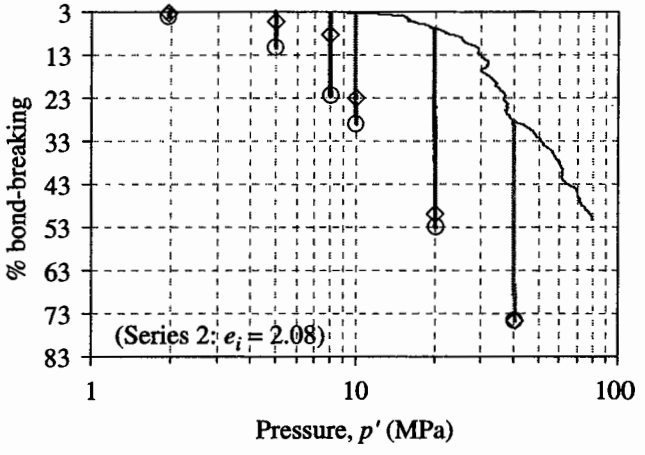

Figure 6. Percentage of bond breakage during isotropic compression and p'-constant shearing (Series 2).

Micro-mechanical data is given in Figure 6, which shows the number of bonds broken after the DEM sample preparation, isotropic compression and the constant-p' shearing stages. Constant-p' shearing caused splitting of grains from a pressure as low as 5MPa, although there were only 3 instances of splitting at 33% deviator strain (30% axial strain). Splitting of grains therefore happens before the pressure reaches critical (8.5 MPa, see Figure 3).

4 LOCATION OF CRITICAL STATE LINE

Figure 7 shows the virgin compression curves from Test Series 1 and 2, and the isotropic unloading path for Test Series 3, compared with lines of critical states. The final state after each constant-p' test is marked and connected with a line for each series. The estimated CSLs for tests starting on the virgin compression lines of denser and looser samples are almost identical. However, the CSL for the over-consolidated series 3 is markedly lower at low stress. This result is important because it shows that the final CSL as originally defined by Schofield & Wroth (1968) is *not unique*, due to variations in particle breakage with the historic maximum stress. Once breakage has permitted grains to repack at lower volume, by small fragments fitting inside previous large voids, it becomes impossible for granular assemblies to regain the high voids ratios of the initial material, however much shearing takes place.

The points of critical pressure from Figures 2, 3 and 4 can also be superimposed on Figure 7, where they are seen to lie above the corresponding lines of final critical states. This is due to the smaller amount of breakage (and the reduced amount of repacking) at the smaller deviator strains associated with p'_{crit}. Once again, the critical pressure for the over-consolidated series 3 samples lies at a smaller voids ratio than those obtained from tests on virgin samples. The critical

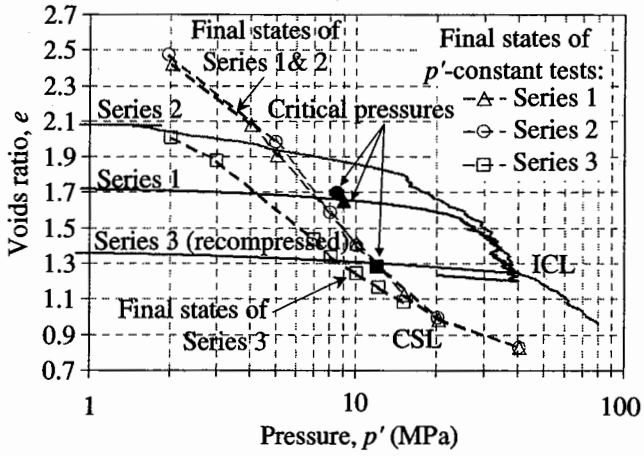

Figure 7. Locations of final states and critical pressures.

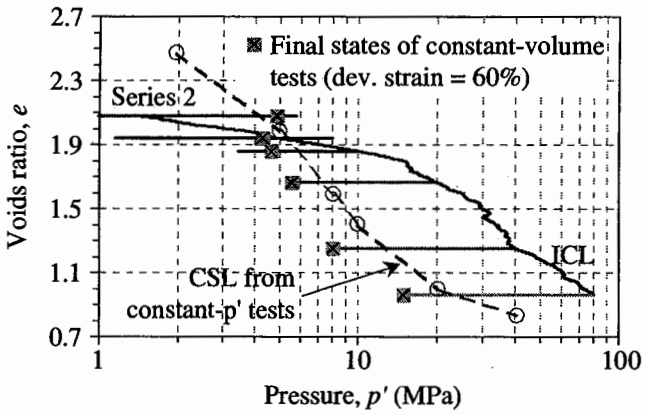

Figure 8. Location of final states predicted from constant-volume tests (Series 2).

pressure changes not only with density and stress level but also with stress history, due to variations in PSD following particle crushing.

5 CONSTANT-VOLUME TESTS

Lade et al. (1996) reported that the particle size distributions obtained after constant-volume (i.e. constant e) tests are different from those obtained from p'-constant tests. The DEM results of constant-e tests on virgin compressed samples are shown in Figure 8. The final critical states are reached after significant amounts of particle breakage, as shown in Figure 9. The CSL is parallel to, and some way below, that defined from the final states of p'-constant tests.

6 FINAL CRITICAL STRESS RATIO

The final stress states, for 60% deviator strain, from all the previous simulations, are shown in Figure 10. There appears to be a unique CSL, but it is not straight. At $p' = 4$ MPa the critical stress ratio $M = q/p' \approx 1.7$,

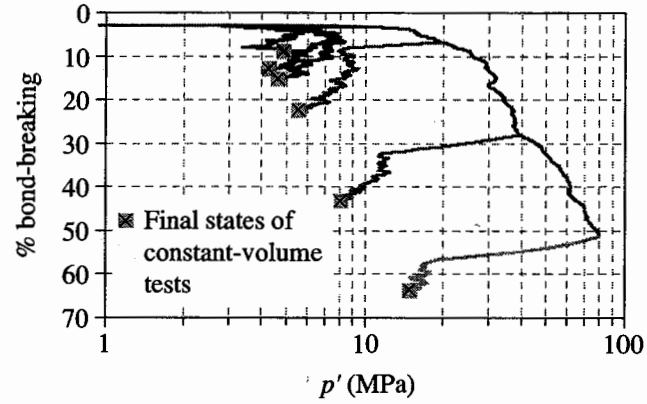

Figure 9. Percentage of bond breakage during isotropic compression and e-constant shearing (Series 2).

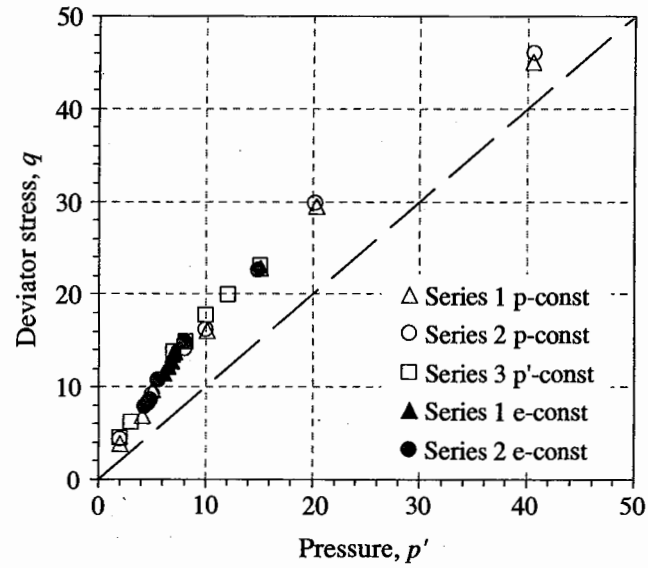

Figure 10. Deviator stress against pressure at final states (60% deviator strain).

corresponding to a Mohr-Coulomb angle of internal friction $\phi_{crit} \approx 42°$, whereas at $p' = 40$ MPa we see $M \approx 1.1$ and $\phi_{crit} \approx 28°$. Although the loss of ϕ_{crit} at high pressure is significant, it may reflect the influence of the particular contact stiffness and grain shape used in these simulations.

7 CONCLUSIONS

DEM clarifies the mechanics of granular soils. Breakage is central not only to elastic-plastic transition, as shown by Cheng et al. (2004), but also to the definition and location of critical states. The critical pressures of p'-constant tests can not be used to exactly locate an ultimate CSL, due to ongoing crushing. The final states obtained from constant-volume tests are also different from those obtained from p'-constant tests, for the same reason. Of greatest significance,

the CSL defined for heavily over-compressed samples lies at voids ratios far below those obtained for virgin samples. No unique line of final critical voids ratios could be found. They varied with stress-path and stress-history. Furthermore, DEM analysis of breakage indicates why, as a matter of principle, this must be the case. Soils with different particle size distributions, due to crushing, have different critical voids ratios. On the other hand, the critical stress ratio was found to depend on the mean stress, but to be independent of stress path.

REFERENCES

Bolton, M.D. 1986. The strength and dilatancy of sands. *Geotechnique* 36(1): 65–78.

Cheng, Y.P. 2004. *Micromechanical investigation of soil plasticity*. PhD thesis, Cambridge University.

Cheng, Y.P., Bolton M.D. & Nakata Y. 2004. Crushing and plastic deformation of soils simulated using DEM. *Geotechnique* 54(2): 131–141.

Cheng, Y.P., Nakata Y. & Bolton M.D. 2003. Discrete element simulation of crushable soil. *Geotechnique* 53(7): 633–642.

Coop, M.R. 1990. The mechanics of uncemented carbonate sands. *Geotechnique* 40(4): 607–626.

Coop, M.R., Sorensen K.K., Bodas Freitas T. & Georgoutsos G. 2004. Particle breakage during shearing of a carbonate sand. *Geotechnique* 54(3): 157–163.

Lade, P.V., Yamamuro, J.A. & Bopp, P.A. 1996. Significance of particle crushing in granular materials. *Journal of Geotechnical Engineering ASCE*, 122(4): 309–316.

Robertson, D. 2000. *Computer simulations of crushable aggregates*. PhD thesis, Cambridge University.

Robertson, D. & Bolton, M.D. 2001. DEM simulations of crushable grains and soils. In: Y.Kishino. (ed.) *Powders and Grains 21–25 May 2001:* 623–626 Netherlands: Balkema.

Roscoe, K.H., Schofield, A.N., & Wroth, M.A. 1958. On the yielding of soils. *Geotechnique* 8: 22–53.

Schofield, A.N. 1980. Cambridge Geotechnical Centrifuge Operations. *Geotechnique* 30(3): 227–268.